A Comparison of AB Diblock and ABA Triblock Copolymers of Polystyrene and Polyferocenylsilane for Nanolithography Applications

by

Juan Carlos Ybarra

Submitted to the Department of Material Science and Engineering
in partial fulfillment of the requirements for the degree of

Bachelor of Science in Material Science and Engineering

at the

MASSACHUSETTS INSTITUTE OF TECHNOLOGY

June 2012

© Massachusetts Institute of Technology 2012. All rights reserved.

Author . . . .
Department of Material Science and Engineering
April 26, 2012

Certified by . . . .
Caroline Ross
Associate Head of the Department of Materials Science and Engineering and the Toyota Professor of Materials Science and Engineering
Thesis Supervisor

Accepted by . . . .
Prof. Jeffrey Grossman
Chair of the Undergraduate Committee

A Comparison of AB Diblock and ABA Triblock Copolymers of Polystyrene and Polyferocenylsilane for Nanolithography Applications

by

Juan Carlos Ybarra

Submitted to the Department of Material Science and Engineering
on April 26, 2012, in partial fulfillment of the
requirements for the degree of
Bachelor of Science in Material Science and Engineering

Abstract

Block coopolymers(BCP) have become of interest in the pursuit novel methods of nanolithography. Their ability to self-assembly into periodic geometries with nanoscale feature sizes makes them attractive as etching masks and templating materials for microelectronics and nanodevices. BCP provide a scalable and low-cost method that is compatible with existing semiconductor fabrication technologies. Though various studies have looked at several combinations of block copolymers we focus on the use of solvent annealing as a method to tune the morphology of PS-b-PFS and PS-b-PFS-b-PS block copolymers. These polymers have shown promise as precursors to a variety of materials and in particular this combination of block copolymers is attractive because we have at our dispossible etching methods with a high selectivity between these two polymers.

Thesis Supervisor: Caroline Ross
Title: Associate Head of the Department of Materials Science and Engineering and the Toyota Professor of Materials Science and Engineering

Acknowledgments

I would like to acknowledge all the encouragement, support, and guidance I received from Professor Caroline Ross. She gave me the opportunity to work on this project that challenged me intellectually and really reinvigorated my interest in academic research. I would also like to thank Adam Floyd Hannon for all of his help, advice, and instruction throughout the course of my work on this project. I would also like to thank William DiNatale for his assitance and advice on SEM imaging.

Contents

1 Introduction **13**

1.1 Overview and Contents 14

1.2 Self-Assembly of Block Copolymers 15

1.2.1 Introduction 15

1.2.2 Phase Separation 16

1.3 Processing Methods for Tuning Block Copolymer Morphology 18

1.3.1 Brush Layers 18

1.3.2 Film Casting Methods 20

1.3.3 Effects of Solvent-Annealing On Domain Spacing 20

2 A Comparison of Morphologies Based on Solvent Annaling of AB Diblock and ABA Triblock Copolymers of Polystyrene and Polyferrocenylsilane **25**

2.1 Introduction 25

2.1.1 Effects of Annealing With Selective Solvents 26

2.2 Observed Morphologies 31

3 Conclusion **37**

List of Figures

1-1 Typical phase diagram for a diblock copolymer a)calculated using consistent mean field theory b)experimentally obtained.[11] 17

1-2 Predicted morphology for bulk diblock copolymers as a function of minority block volume fraction.[11] 17

1-3 Observed morphologies for lamellar forming diblocks for a)large disparity in preference for substrate or air interface b) small disparity in preference for substrate or air interface.[1] 19

2-1 The maximum swelling of PFS homopolymer for 6 solvent annealing conditions with increasing partial pressure of toluene. For a normalized partial pressure of zero, 10 SCCM of chloroform was used to anneal the samples. The 4 speeds are the range of RPM used to spin coat the PFS on to silicon samples approximately 1 cm^2. 28

2-2 The maximum swelling of PS homopolymer for 6 solvent annealing conditions with increasing partial pressure of toluene. For a normalized partial pressure of zero, 10 SCCM of chloroform was used to anneal the samples. The 4 speeds are the range of RPM used to spin coat the PFS on to silicon samples approximately 1 cm^2. 29

2-3 The maximum swelling of PS-b-PFS for 6 solvent annealing conditions with increasing partial pressure of toluene. For a normalized partial pressure of zero, a ratio of 8 SCCM of chloroform to 2 SCCM of nitrogen gas was used to anneal the samples. The error bars represent 1 standard deviation. 29

2-4 The maximum swelling of PS-b-PFS-b-PS for 6 solvent annealing conditions with increasing partial pressure of toluene. For a normalized partial pressure of zero, a ratio of 8 SCCM of chloroform to 2 SCCM of nitrogen gas was used to anneal the samples. The error bars represent 1 standard deviation. 30

2-5 Thermally annealed PS-b-PFS sample with an equilibrium period of $37 \pm 2nm$.Samples with an inital thickness of 50nm were annealed at 180 degrees Celcius for a few hours. 31

2-6 Thermally annealed PS-b-PFS-PS sample with an equilibrium period of $26 \pm 1nm$.Samples with an inital thickness of 50nm were annealed at 180 degrees Celcius for a few hours. 32

2-7 Comparison of PS/PFS diblock and triblock solvent annealed using 10 SCCM toluene or 22 torr toluene. 33

2-8 Comparison of PS/PFS diblock and triblock solvent annealed using 8 SCCM toluene:1.6 SCCM chloroform:0.4 SCCM nitrogen gas or 17.4 torr toluene:40.9 torr chloroform 33

2-9 Comparison of PS/PFS diblock and triblock solvent annealed using 4 SCCM toluene:4.8 SCCM chloroform: 1.2 SCCM nitrogen gas or 8.5torr toluene:120.4 torr chloroform 34

2-10 Comparison of PS/PFS diblock and triblock solvent annealed using 8 SCCM chloroform:2 SCCM nitrogen gas or 196 torr chloroform . . . 34

2-11 49kg/mol 42% PFS by volume PS-b-PFS sampled thermally annealed. 35

List of Tables

2.1 Solvent annealing conditions according to ratio of toluene to chloroform to nitrogen. 28

Chapter 1

Introduction

The self-assembly of molecules into well ordered systems with hierarchical structure is at the core of many phenomena in condensed matter including life itself. With our ever expanding knowledge of microscale and nanoscale forces that govern these phenomena we will be able to understand how to direct this self-assembly for specific industrial applications. In modern industrial microelectronics and various other nanodevices require nanoscale feature sizes. These high resolution features sizes must be achieved with technologies that yield high throughput while producing both long range order and arbitrary strutures with a low defect density[1]. For any method to be viable in industry this high throughput of high quality patterning must be scalable and cost effective. Modern optical lithography meets all these criteria. However,the features sizes produced by optical lithography are limited by the wavelength of light used. One of the earliest alternatives proposed has been electron beam lithography (EBL). EBL is not difftaction limited, instead the resolution of electron beams are controlled by optical systems that can vary the accelerating voltage and the beam shape and size. So EBL is capable of producing highly resolved features in the nanometer range. Its high resoltion capabilities have made it an excellent method for producing lithographic masks for optical lithography. The ultimate resolution of EBL is determined by the resolution of the resist and the subsequent fabrication processes.[2] For example, experiments with a hydrogen silsesquioxane (HSQ) photoresist developed with an aqueous alkali solution of tetramethyl ammonium hydroxide was shown to

produce a minimum feature size of 4.5 nm.[3] The disadvantage of this method is that patterns are typically defined serially which leads to a relatively low throughput.[1, 4] Similar methods such as ion beam and neutral particle lithography share this same disadvantage. Other early methods proposed have been optical lithography using extreme ultra violet light (EUV) and X-rays. These optical methods have their own advantages and disadvantages related to optimization of the materials used and optical systems that are of interest to the modern semiconductor fabrication industry but shall not be discussed here. Greater demand for higher resolution features has impelled scientists to search for new methods of fabrication. Some proposed methods have been nanoimprint lithography[5], and self-assembled block copolymers[6]. Each of these methods have advantages and disadvantages compared to optical lithography being used in the semicondictor fabrication and other modern large scale micro/nano device fabrication. They are all developing and improving but here I shall focus on self-assembled block copolymers (BCP). BCP film casting and processing is low cost and scalable in addition to being compatible with existing semiconductor fabrication. BCP are capble of forming period arrays of self-assembled, well defined nanoscale features. When coupled with selective etching of one or more blocks, these periodic arrays of dots, holes, and lines (in plane cylinders) can be used as masks for fabrication of nanoscale structures and devices.[9,10,11]

1.1 Overview and Contents

Chapter 1. In subsequent sections I shall explain the thermodynamic driving forces for self-assembly.I then describe some of the processing methods that exploit these driving forces for tuning the morphology and ordering of block-copolymer thin films, focusing on those methods used in our own study. Looking at the various solvent and surface treatments will help us understand what other directions can be taken to expand the functionality of block copolymer systems.

Chapter 2. In this chapter I will use a polystyrene-polyferrocenylsilane diblock (ps-b-pfs) and polystyrene-polyferrocenylsilane-polystyrene triblock (ps-b-pfs-b-ps) to

contrast the use of AB diblock and ABA triblock copolymers.

Chapter 3. The chapter will give an overview of future work that will expand upon the experiements conducted in this study, specifically the use of ABA triblocks for nanolithography.

1.2 Self-Assembly of Block Copolymers

1.2.1 Introduction

A polymer is composed of a repeating molecular unit, or monomer. Copolymers are composed of two distinct monomers that can be arranged in random, alternating, or block patterns. These copolymers are capable of forming various geometrical arrangements, such as star, comb, brush, ladder, or dendritic architectures. Block copolymers have been used in wide variety of industrial applications, such as solubilizers, compatibilizers, foams, oil additives, and as thermoplastic elastomers.[10] Here I will focus on applications of linear block copolymers because they can be induced to undergo nanoscale self-organization into periodic composition patterns. [11] Linear block copolymers are typically synthesized using living anionic polymerization. In this method of polymerization an akali metal or alkaline earth metal is reacted with the initial monomer to create a reactive carbanionic site that initiates chain propagation. These are called "living" reactions because there is an absence of an inherent termination process. This means that as long as there is a supply of monomer the polymer chain will always continue to grow. Under careful control of conditions this method allows for a predefined molar mass and a nearly ideal polydispersity [1, 11]. Polydispersity is the measure of the overall distribution of molecular weights of the synthesized polymer chains. This is quantified by the polydispersity index (PDI) given by,

$$PDI = \frac{M_w}{M_n}$$

This method is the most convenient way of producing block copolymers because the terminal active site of one polymer chain can be used to initiate the polymerization

of a different monomer creating two, or more, distinct blocks.

1.2.2 Phase Separation

Block copolymers that undergo microphase separation are driven by the chemical incompatibility between the different blocks that the copolymer is composed of. This leads to opposing thermodynamics effects. At lower temperatures, enthalpic effects dominate driving phase separation, while at higher temperatures, entropy dominates driving the polymers towards homogenous mixing. Phase separation will occur when the Gibbs free energy of mixing is greater than 0. The Gibbs free energy of mixing for two homopolymers is given by the Flory-Huggins equation

$$\frac{\Delta G_{mix}}{k_b T} = \frac{\phi_A}{N_A}\ln(\phi_A) + \frac{\phi_B}{N_B}\ln(\phi_B) + \phi_A\phi_B\chi$$

where ϕ, N, and χ are the volume fraction, degree of polymerization, and Flory-Huggins interaction parameter, respectively. The Flory-Huggins interaction parameter is related to the enthalpic change due to the incompatibility of the two different monomer units. In general its temperature dependence is

$$\chi = \frac{a}{T} + b$$

where a and b are experimentally determined constants for a given composition of BCP.

An important parameter for determining phase separation is the segregation strength found by taking the product χN. The segregation strength reflects enthalpic and entropic contributions. When χN is smaller than a certain value at a given composition then the chains will be homogenously mixed in a disordered state. For a symmetric diblock, mean field theory calculations yield a order-disorder transition (ODT) value of 10.5. Values of $10.5< \chi N<12$ corresponds to the weak segregation limit (WSL), in this regime the composition profile is sinusoidal. The strong segregation limit (SSL) occurs at values of $\chi N>>10.5$. In this regime the composition profile is close to a square function and the interfaces are much more narrow as compared

to the WSL. The interfacial width and domain spacing in the SSL scale as $\frac{a}{\sqrt{\chi}}$ and a$N^{1/3}\chi^{1/6}$, respectively.[1,11] For χN below the ODT the block copolymer system will microphase separate into a body-centered cubic arrangement of spheres, hexagonally-packed cylinders, bicontinuous cubic gyroid, or lamellar phases depending on phase fraction. In the WSL χN may affect the microstructure of the BCP, but in the SSL the phase fraction is a much more important factor.[11] Using self-consistent mean field theory (SCMFT) to predict which morphologies will be produced for a particular phase fraction typically produces symmetric phase diagrams. Experimental results show a more distorted shape due to dissimilarities in the stereochemistry and chain conformation of type A and type B monomers of a particular diblock.[[1]] Other factors such as non-uniform chain stretching, realistic distributions of chain ends and block junctions, and non-uniform χ also cause this distortion though some models account for these factors.[13]

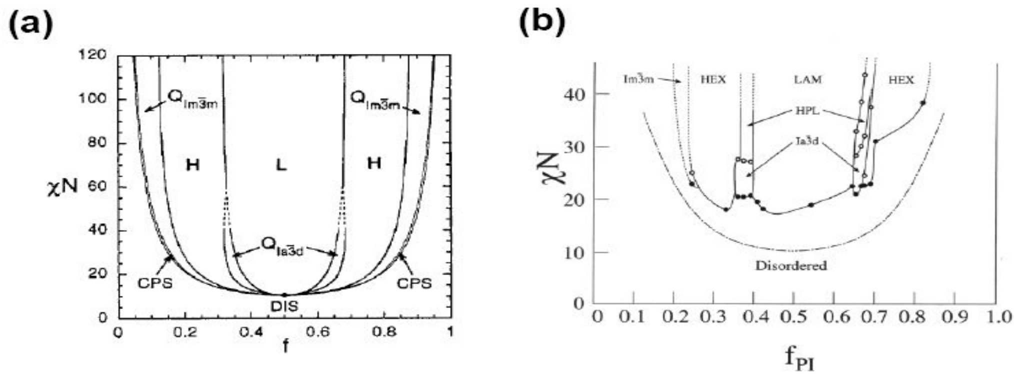

Figure 1-1: Typical phase diagram for a diblock copolymer a)calculated using consistent mean field theory b)experimentally obtained.[11]

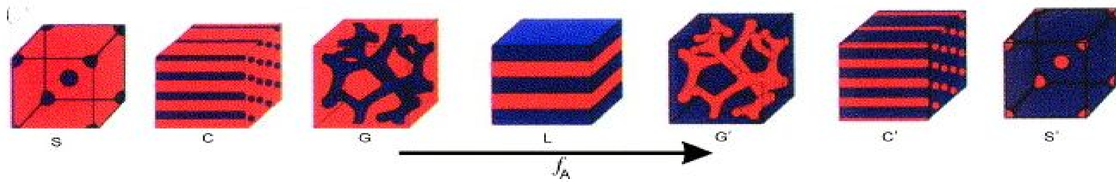

Figure 1-2: Predicted morphology for bulk diblock copolymers as a function of minority block volume fraction.[11]

The above geometries are determined for bulk materials. For many applications,

specifically lithography, thin films are desired. In lithographic applications monolayers are used as templates or etch masks. For spin coating of the polymer film on a substrate, the thickness of the film is controlled by concentration of the solution and the spin speed used. For thin films the observed morphology is affected by the film thickness, equilibrium period, and boundary conditions at the substrate-polymer and air-polymer interfaces. The equilibrium thickness is affected by the chain length and processing conditions. For example in lamellar structures, there are four possible configurations. If the thickness of the film is equal to the equilibrium thickness, the structure will form uniform lamellae that are parallel to the surface, regardless of interfactial energy considerations. One block may prefer to be at either the substrate or air interface but this will not affect the geometry. If the thickness is greater than the equilibrium thickness, but there is a strong prference for one of the blocks to minimize its surface energy at either the substrate or air interface terracing will occur. For thicknesses less than the equilibrium thickness, and strong preference for a particular interface, hole and island formation will occur. If the preference for either the air or substrate interfaces is the same for each block, lamellae perpendicular to the surface will form for thicknesses greater than or less than the equilibrium thickness.[1]

1.3 Processing Methods for Tuning Block Copolymer Morphology

The complexity of BCP systems results in many parameters which can be adjusted in order to control the compostion and morphology of the BCP system for a particular purpose. Here I discuss how some of the boundary conditions and processing methods can be adjusted in order to control the periodicity and morphology of BCP thin films.

1.3.1 Brush Layers

Each block may have a preference for either the air or substrate interface. If bare silicon is used, strong interactions between the native oxide of bare silicon and one or

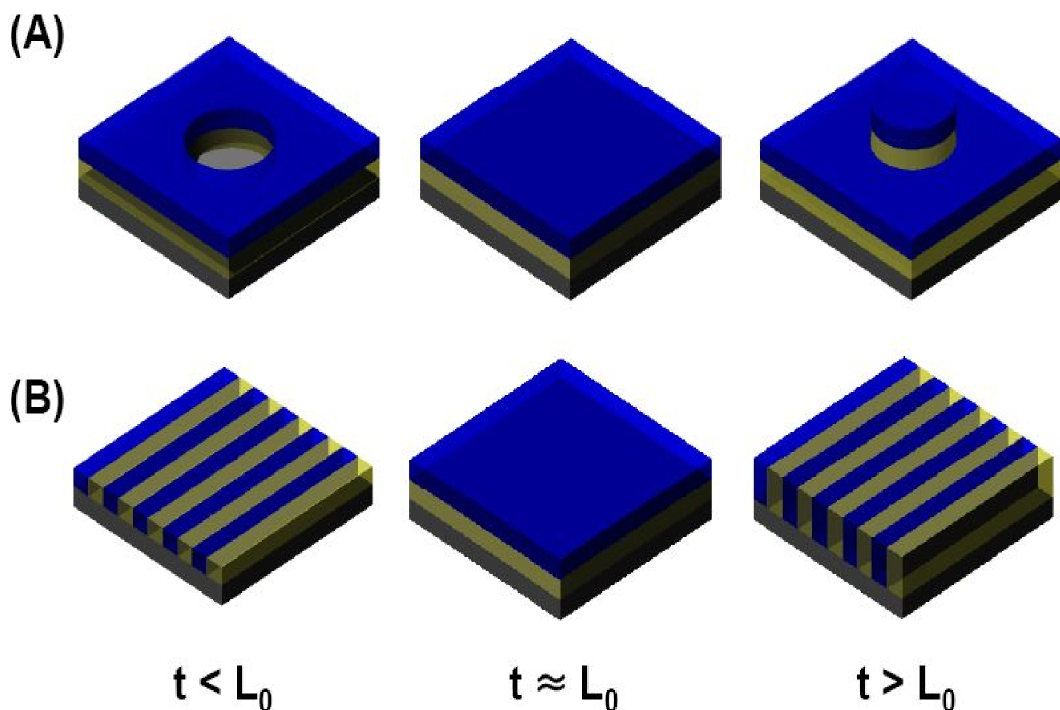

Figure 1-3: Observed morphologies for lamellar forming diblocks for a)large disparity in preference for substrate or air interface b) small disparity in preference for substrate or air interface.[1]

more blocks may impede diffusion.[1] This will lead to a disordered state. Brush layers can not only prevent such strong interactions but also improve the ordering of a particular morphology. For example, we can consider a polystrene-polydimethylsiloxane diblock copolymer (PS-b-PDMS). The surface energies γ for the the polymers are $\gamma_{PDMS} = 19.9\frac{mN}{m}$ and $\gamma_{PS} = 40.7\frac{mN}{m}$.[14]. If the brush layer is composed of the majority block the preference for the majority block to interact with the substrate leads to a thinner equilibrium thickness, L_0.[15] This means that if a film thickness close to the equilibrium film thickness observed in samples with a minority block brush layer is spin coated, a sample with a majority block brush of equal thickness will exhbibit terracing (observed as island formations).[15] The ability of the majority block to increase ordering depends on γ. In a study by C. Harrison, et al. a PDMS minority block layer increased ordering by allowing greater diffusion of polymer chains.[14,15]

1.3.2 Film Casting Methods

It is important to note that the method by which a film is cast may affect its properties. X. Zhang, et al have shown that flow-coating of polymer films creates higher residual stress by stretching polymer chains in non-equilibrium conformations. However this method can also be used to alter the orientation of BCP. In their study PS-b-PMMA blocks exhibited in plane cylinders if spin coated and cylinders perpendicular to the surface if flow coating is used.[16] They also showed that film casting speed has no effect on residual stress and morphology for polymer films of equal thickness.[16]

1.3.3 Effects of Solvent-Annealing On Domain Spacing

Solvent annealing has been shown to be an effective tool in tailoring the morphology of BCP. We can use solvent vapor pressure and various ratios of selective and partially selective solvents in order to control BCP morphology.[1,17,18] Increasing vapor pressure will increase the degree of solvent uptake in the film. Increasing solvent uptake will increase chain mobility and decrease interfacial interactions between blocks. This change in interfacial interactions between the blocks alters χ such that the effective Flory-Huggins parameter χ_{eff} can be calculated as

$$\chi_{eff} = \chi(1 - \phi_s)$$

where ϕ_s is the volume fraction of solvent in the film. The χ_{eff} alters the free energy of the polymer system. In the SSL, there is a balance of free energy due to stretching of polymers upon phase separation and the formation of a surface between polymer microdomains. The stretching of a polymer chain decreases the configurational entropy and the formation of a surface increases the enthalpy. If we decrease the enthalpic penalty of creating a surface we see a decrease in the period of our BCP. The entropy of stretching in this case is

$$\Delta S = \frac{-k_b}{2}(\alpha_x^2 + \alpha_y^2 + \alpha_z^2 - 3)$$

where α is the ration of the stretched length to the original length. Assuming constant volume $\alpha_x \alpha_y \alpha_z = 1$, only considering stretching in the x direction, and taking α_x to be transverse to the interface between two microdomains, the relationship between the period λ and entropy is

$$\Delta S = \frac{-k_b}{2}[(\frac{\lambda}{\lambda_0})^2 + 2\frac{\lambda}{\lambda_0} - 3]$$

From this equation we see that the enthalpic penalty for creating a surface is the product of the interfacial energy γ and the contact area per chain Σ. The interfacial energy is given by

$$\gamma = \frac{k_b T}{a^2}\sqrt{\frac{\chi_{eff}}{6}}$$

where a is the Kuhn length (average length of a monomer unit of the polymer). Thus the free energy is

$$\Delta G = \gamma\Sigma + \frac{-k_b}{2}T[(\frac{\lambda}{\lambda_0})^2 + 2\frac{\lambda}{\lambda_0} - 3]$$

and finding the minimization of this function gives us our domain spacing[19,20].

[1] Yeon Sik Jung. Templated Self-Assembly of Siloxane block copolymers for nanofabrication. Ph.D. Thesis. Massachusetts Institute of Technology, Cambridge, MA, U.S.A., 2009. [2] A.N. Broers, A.C.F. Hoole, 1.M. Ryan.Electron beam lithography - Resolution limits. Microelectronic Engineering 32 (1996) 131-142.

[3]Joel K. W. Yang, Bryan Cord, Huigao Duan, and Karl K. Berggren Joseph Klingfus Sung-Wook Nam, Ki-Bum Kim, Michael J. Rooks. Understanding of hydrogen silsesquioxane electron resist for sub-5-nm-half-pitch lithography. J. Vac. Sci. Technol. B 27(6), Nov/Dec 2009.

[4] McCord, M. A.; M. J. Rooks (2000). "2". SPIE Handbook of Microlithography, Micromachining and Microfabrication.

[5] Stephen Y. Chou,a) Peter R. Krauss, Wei Zhang, Lingjie Guo, and Lei Zhuang. Sub-10 nm imprint lithography and applications. J. Vac. Sci. Technol. B 15.6.,Nov/Dec 1997.

[6] Frank S. Bates and Glenn H. Fredrickson. Block Copolymer Thermodynamics: Theory and Experiment. Annual Review of Physical Chemistry, Vol. 41: 525 -557. October 1990.

[7] Jung YS, Jung W, Tuller HL, Ross CA. Nanowire conductive polymer gas sensor patterned using self-assembled block copolymer lithography. Nano Lett. 2008 Nov;8(11):3776-80. Epub 2008 Oct 28.

[8] Rachel A. Segalman. Patterning With Block Copolymer Thin Films. Materials Science and Engineering R 48 (2005) 191-226

[9] Jin Kon Kim, Seung Yun Yang, Youngmin Lee, Youngsuk Kim. Functional nanomaterials based on block copolymer self-assembly. Progress in Polymer Science 35 (2010) 1325-1349

[10] A.K. Kandpur, S. Forster, F.S. Bates, et al. Polyisoprene-polystyrene Diblock Copolymer Phase Diagram Near the Order-Disorder Transition. Macromolecules, 28 (1995) 8796-8806.

[11] Frank S. Bates and Glenn H. Fredrickson. Block Copolymers-Designer Soft Materials. Phys. Today 52(2), 32 (1999)

[12] R.J. Young and P.A. Lovell. Introduction To Polymers. 2nd Edition. New York: CRC Press, 1991.

[13] Frank S. Bates and Glenn H. Fredrickson. Block Copolymer Thermodynamics: Theory and Experiment. Annual Review of Physical Chemistry, Vol. 41: 525 -557. October 1990.

[14] S. J. Clarson and J. A. Semlyen, "Siloxane Polymers," PTR Prentice Hall, New Jersey., 1993, pp 567-615.

[15] C. Harrison, P. M. Chaikin, D. A. Huse, R. A. Register, D. H. Adamson, A. Daniel, E. Huang, P. Mansky, T. P. Russell, C. J. Hawker, D. A. Egolf, I. V. Melnikov, E. Bodenschatz. Reducing substrate pinning of microdomains with a buffer layer of polymer brushes. Macromolecules, Vol. 33 (2000)

[16] Xiaohua Zhang, Jack F. Douglas, and Ronald L. Jones. Influence of film casting method on block copolymer ordering in thin films. Soft Matter, 2012,8, 4980-4987

[17] J.K. Bosworth, "Control of Self-assembly of lithographically patternable block copolymer films" Acs Nano 2, p.1346 (2008)

[18] J. Bang. "Effect of humidity on the ordering of PEO-based copolymer thin films. Macromolecules 40, P. 7019, 2007.

[19] E. Helfand, Y. Tagami. Theory of the interface between two immiscible polymers. II. Journal of Chemical Physics 56, p.3592 (1972)

[20] R.J. Young and P.A. Lovell. Introduction To Polymers. 2nd Edition. New York: CRC Press, 1991.

Chapter 2

A Comparison of Morphologies Based on Solvent Annaling of AB Diblock and ABA Triblock Copolymers of Polystyrene and Polyferrocenylsilane

2.1 Introduction

The growing demand for nanoscale fabrication methods has motivated research into novel techniques for nanofabrication. The scalable and low-cost method of block copolymer self-assembly has been investigated in order to optimize the processing parameters for various functional materials and devices. Block copolymers are capable of producing periodic arrays which, combined with grapheoepitaxy or other methods, may be capable of long-range order with low defect density[1]. The self-assembled block copolymers may be used as lithographic masks or templates for other materials[2,3]. In the previous chapter we discussed some of the methods used to tune the morphology of self-assempled BCP systems. For our experiments we spin

coated thin films of polystyrene-polyferrocenylsilane diblock copolymer (PS-b-PFS) and a polystyrene-polyferrocenylsilane-polystyrene triblock copolymer (PS-b-PFS-b-PS)onto a silicon substrate coated with PS brush layer (PS being the majority block). A PS brush layer was chosen because we assumed that it would promote ordering and packing of the PFS block in the PS matrix for our triblock system. We believe that using a PFS brush for the triblock system would cause the BCP to fold and have the PS ends come together near the air-polymer interface. Future investigation may be needed to confirm this assumption. Reactive-ion ethching (RIE) is used in order to image our samples. One attractive feature of this BCP system is the exploitation of the high etch resistance of PFS nanodomains with respect to its surrounding matrix. In previous studies the etch resistance of PFS has been exploited in order to nanopattern surfaces.[4] Some of the other attractive properties include interesting redoxactivity (associated with the reversible Fe(II)/Fe(III) couple), semi-photoconductivity,and an ability to act as a magnetic ceramic or catalyst precursor. [5]

2.1.1 Effects of Annealing With Selective Solvents

In order to study the effects of selective solvents on the swelling of each block we first studied the effects of selective annealing on PS homopolymer and PFS homopolymer in various ratios of mixed chloroform, toluene, and nitrogen gas vapor. We then compared these data with results from PS-b-PFS and PS-b-PFS-b-PS solvent annealed under the same conditions. We looked at the relative swelling for each sample and the annealing time in order to determine a swelling rate which we can then correlate to a particular morphology. From the Hildebrand solubility parameters δ we expected partially selective swelling of PS ($\delta_{PS} = 18.5MPa^{1/2}$)[6] by toluene ($\delta_{toluene} = 18.2MPa^{1/2}$)[7] and PFS($\delta_{PFS} = 18.7MPa^{1/2}$)[8] by chloroform($\delta_{chloroform} = 19.0MPa^{1/2}$)[7]. When solvent annealing our samples we held the flow rate constant at 10 SCCM. The relationship between the volumetric and molar flow rates of the solvents is given by

$$q = Q\frac{\rho}{M}$$

where q is the molar flow rate, Q is the volumetric flow rate in SCCM, ρ is the density of the solvent, and M is the molar mass. Assuming a mixture of ideal gases, Raoult's law says that the molar percent of each gas is approximately equal to the percent partial pressure of each gas.[6] For each solvent the pressure can be written as

$$p_{solvent} = p^*_{solvent}(\frac{q_{solvent}}{q_{total}})$$

where $p^*_{solvent}$ is the saturation vapor pressure of a solvent at particular conditions (in our case this is at 1 atm and 298.15K) and q_{total} is the sum of the molar flow rates for each solvent during solvent annealing.[6] In this study we solvent annealed PS-b-PFS and PS-b-PFS samples with volume fractions $\phi_{PFS} = 0.42$ and $\phi_{PS} = 0.58$ using various ratios of toluene, chloroform, and nitrogen while maintaining a constant flow rate. For the diblock the chain simply has a block structure with volume fractions 0.42PFS/0.58PS and for the triblock sample this ends up being a 0.28PS/.42PFS/0.28PS block structure. We used 58 kg/mol diblock and a 45kg/mol triblock. Below is a list of the solvent annealing conditions used in this study as well as swelling data obtained for these conditions. It should be noted that for all studies the first 5 ratios are constant. For the homopolymer studies 10 SCCM chloroform was used and for the diblock and triblock increasing partial pressure of chloroform lead to increased dewetting of samples. To limit dewetting the partial pressure of chloroform to nitrogen gas was decreased to 8SCCM chloroform to 2 SCCM nitrogen to prevent dewetting of samples which can hinder SEM imaging of morphologies.

For each solvent annealing condition samples are placed on a glass slide and sealed within the solvent annealing chamber.Using ultraviolet-visible spectrophotometry (UV-Vis), we compare the acquired spectra with that of a silicon wafer coated with a PS brush layer in order to determine the initial thickness of the films spin coated on each sample. Gas consisting of one of the solvent mix ratios, A through G, then flows into the chamber. After allowing 15 minutes for the gas in the chamber to reach an equilbrium vapor pressure, the thickness of the samples are measured again using UV-Vis. We continue to measure the thickness of the films every 10 minutes.

Table 2.1: Solvent annealing conditions according to ratio of toluene to chloroform to nitrogen.

Condition	Toluene	Chloroform	Nitrogen (N_2)	Toluene (torr)	Chloroform (torr)
A	10	0	0	22	0
B	8	1.6	0.4	17.4	40.9
C	6	3.2	0.8	12.9	81.2
D	4	4.8	1.2	8.5	120.4
E	2	6.4	1.6	4.2	159.0
F	0	8	2	0	196
G	0	10	0	0	196.7

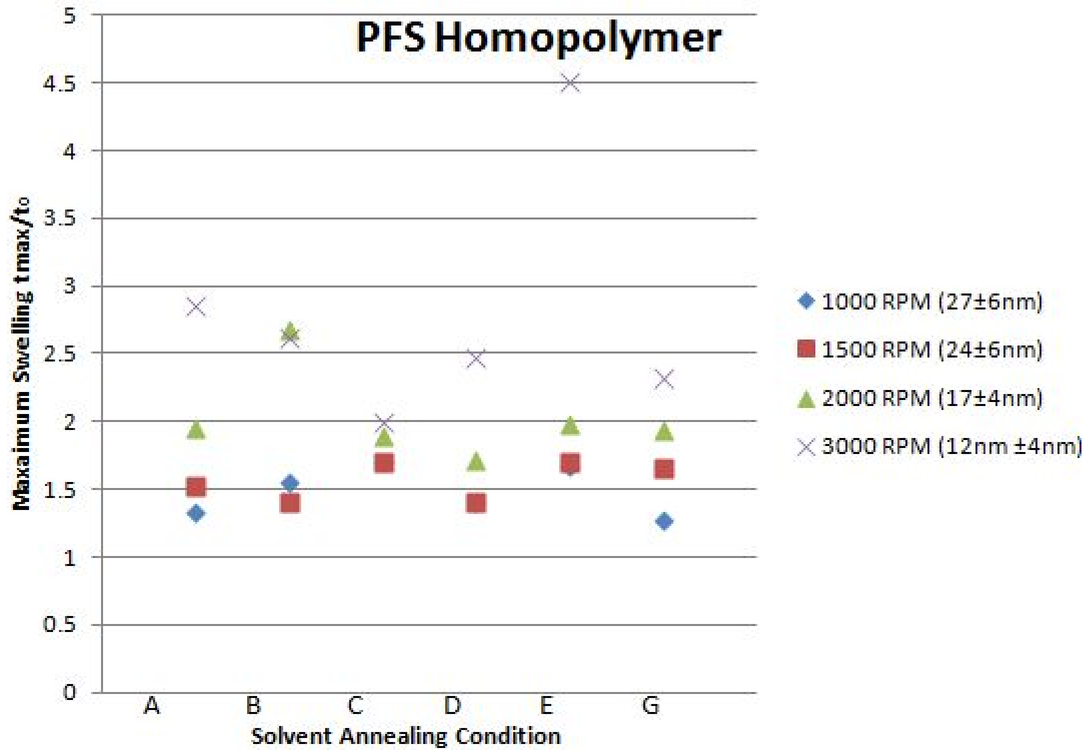

Figure 2-1: The maximum swelling of PFS homopolymer for 6 solvent annealing conditions with increasing partial pressure of toluene. For a normalized partial pressure of zero, 10 SCCM of chloroform was used to anneal the samples. The 4 speeds are the range of RPM used to spin coat the PFS on to silicon samples approximately 1 cm^2.

In figures 2.1 and 2.2 we see that there is little correlation between the partial pressures of toluene and chloroform and the maximum swelling of either PFS or PS homopolymer. We see similar results in both the diblock and triblock cases in figures

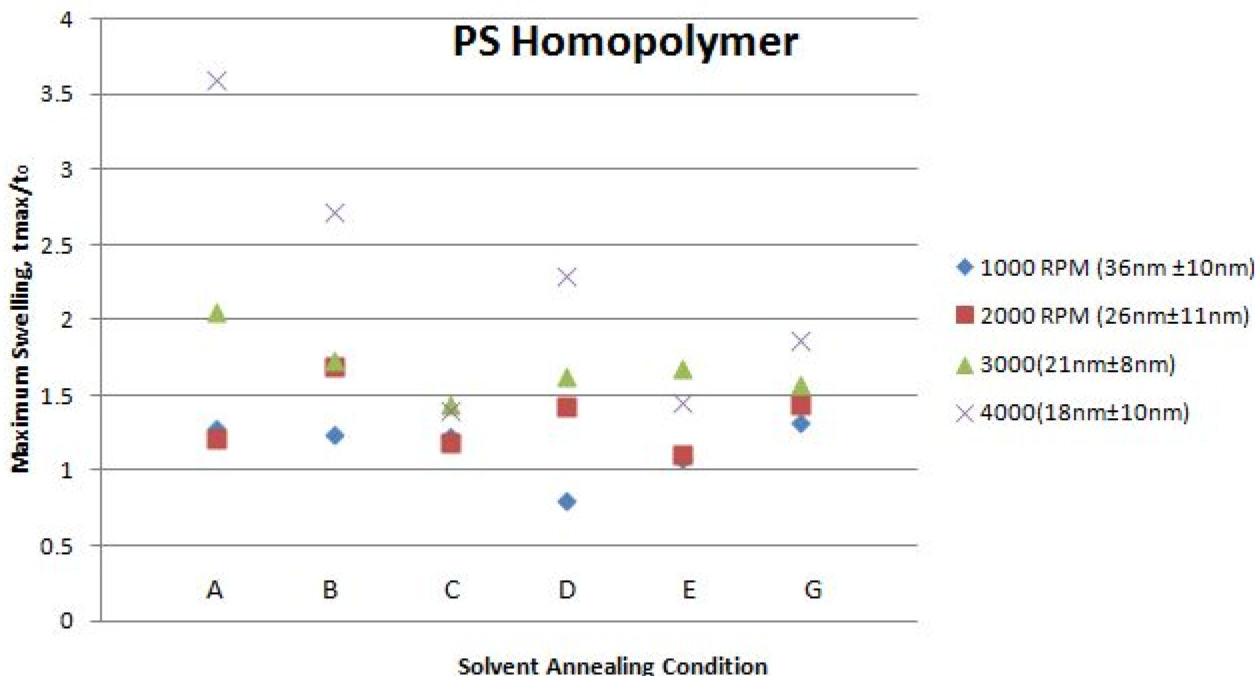

Figure 2-2: The maximum swelling of PS homopolymer for 6 solvent annealing conditions with increasing partial pressure of toluene. For a normalized partial pressure of zero, 10 SCCM of chloroform was used to anneal the samples. The 4 speeds are the range of RPM used to spin coat the PFS on to silicon samples approximately 1 cm^2.

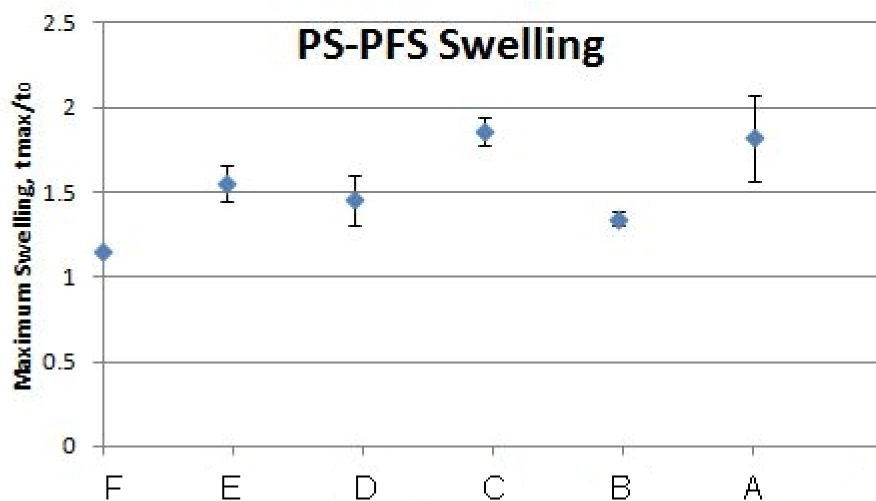

Figure 2-3: The maximum swelling of PS-b-PFS for 6 solvent annealing conditions with increasing partial pressure of toluene. For a normalized partial pressure of zero, a ratio of 8 SCCM of chloroform to 2 SCCM of nitrogen gas was used to anneal the samples. The error bars represent 1 standard deviation.

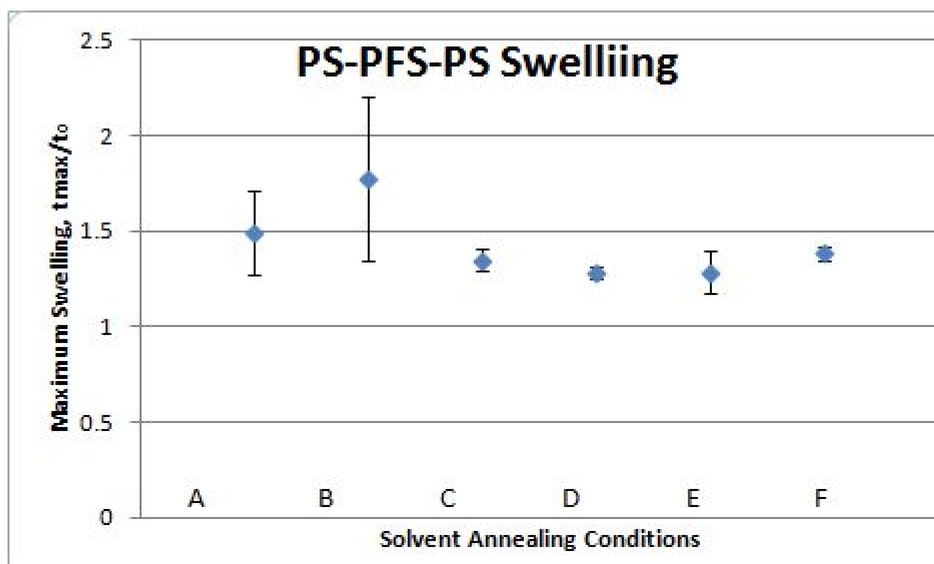

Figure 2-4: The maximum swelling of PS-b-PFS-b-PS for 6 solvent annealing conditions with increasing partial pressure of toluene. For a normalized partial pressure of zero, a ratio of 8 SCCM of chloroform to 2 SCCM of nitrogen gas was used to anneal the samples. The error bars represent 1 standard deviation.

2.3 and 2.4, respectively. From figures 2.1 and 2.2 the PFS homopolymer and PS homopolymer samples show greater swelling in the samples spin coated at higher speeds. We believe that solvent uptake was greater in the thinner samples because the solvent has a shorter distance of polymer through which it must diffuse. For the diblock and triblock samples we maintained a range of spin coating speeds that correlated to a thicknesses in the range of equilibrium periodicities L_0 found from previous work with PS-b-PFS ($L_0 = 26 \pm 1nm$) and PS-b-PFS-b-PS($L_0 = 37 \pm 2nm$) thin films.

The annealing time at which maximum thickness can be achieved was experimentally determined by observing the thickness at which dewetting of the surface becomes obvious. For our thinner, triblock samples this could be observed visually as the formation of islands that are visible to the naked eye. This typically correlates to the annealing time at which the thickness appears to level off or in some cases we see a sudden drop in thickness. For the diblock samples we typicallly see a leveling off of the thickness 35 - 45 minutes after solven annealing has begun until the ratio of Chloroform is greater than 3.2 SCCM, For samples with a greater partial pressure

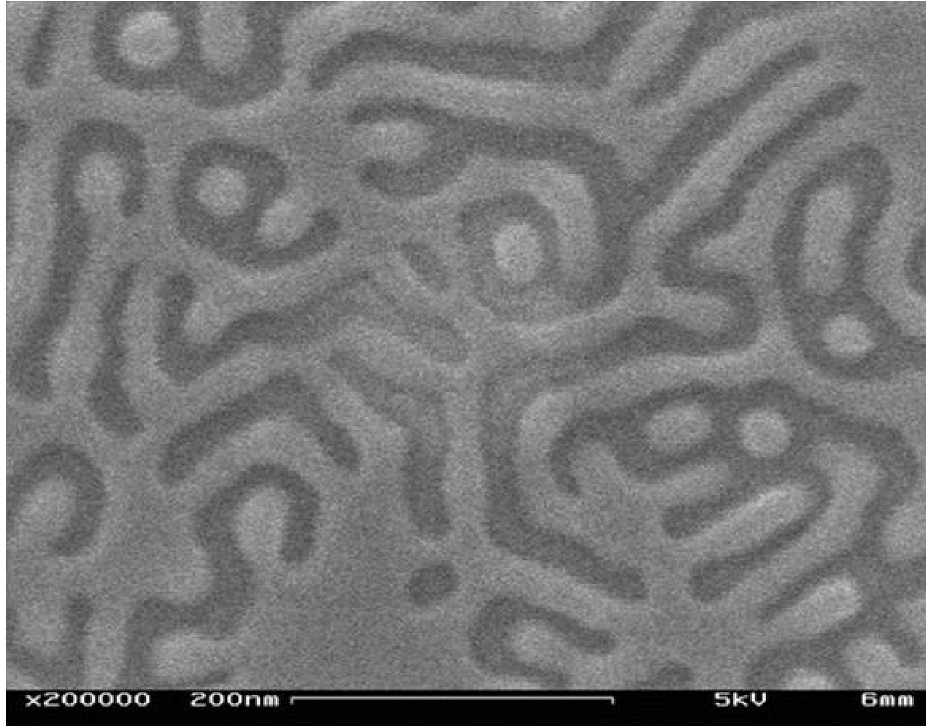

Figure 2-5: Thermally annealed PS-b-PFS sample with an equilibrium period of $37 \pm 2nm$.Samples with an inital thickness of 50nm were annealed at 180 degrees Celcius for a few hours.

of chloroform we typically see leveling off occur 25-35 minutes after solvent annealing has begun. For the triblock samples with larger ratios of toluene there is typically a sudden drop in thickness 25 -35 minutes into solven annealing and for ratios of chloroform with 3.2 SCCM or greater this can occur 15 - 25 minutes after solvent annealing has begun. This is expected since the triblock samples are thinner and thus will have greater solvent uptake.

2.2 Observed Morphologies

After solvent annealing each sample was etched using reactive-ion etching (RIE) with oxygen plasma and then were imaged via a scanning electron microscope (SEM). From these images we see that on average the periodicity of the triblock samples is less than that of the diblock samples. For a bulk diblock copolymer sample with a 42% of the minority block, a gyroid structure is the equilibrium morphology. For the

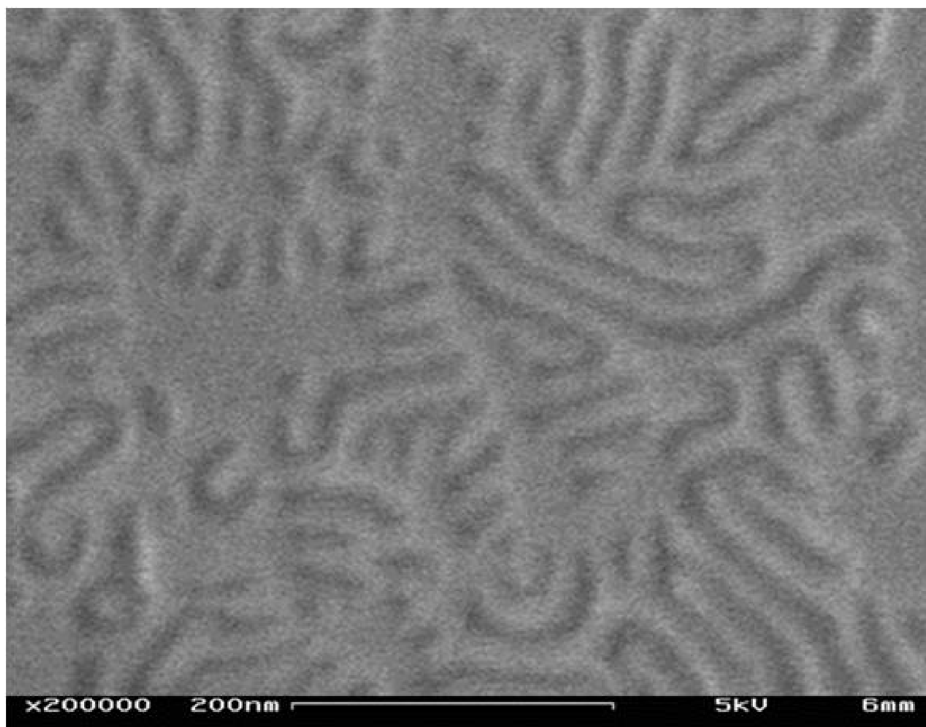

Figure 2-6: Thermally annealed PS-b-PFS-PS sample with an equilibrium period of $26 \pm 1nm$.Samples with an inital thickness of 50nm were annealed at 180 degrees Celcius for a few hours.

sample which was annealed using 10 SCCM toluene both the triblock and diblock exhibit this morphology. However as the ratio of chloroform to tolune is increased there is a shift towards cylindrical and spherical morphologies. For the diblock this appears as in plane cylinders. However for the triblock sample we see what may be either micelles or inplane lamellae with a circular shape. Further investigation is necessary to determine the actual morphology. These circular features show a high polydispersity, showing that they are less ordered than the diblock sample. This may be due to the fact that the triblock samples are thinner and therefore have a greater solvent uptake. During solvent annealing it was noted that the triblock samples show greater dewetting earlier on due to this greater solvent uptake. This dewetting may prevent further ordering that would occur if the solvent annealing could be carried out over as long a duration as in the diblock samples. Furthermore, if PS-PFS systems are to be used as lithographic masks or templates they would require greater long range order. The first step in inducing greater order would be to use solvents with

toluene ps pfs up close.jpg

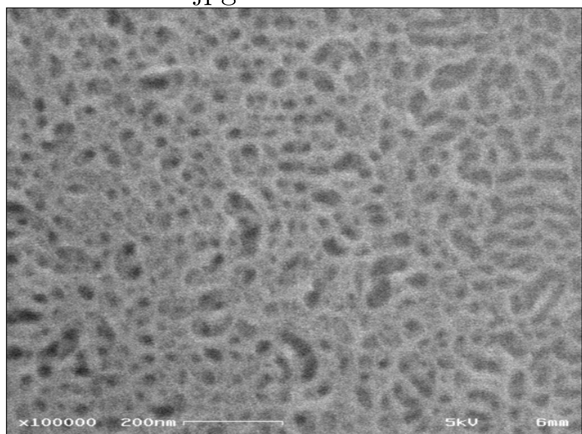

(a) ps-b-pfs with inital thickness of 36 nm

ps pfs ps.jpg

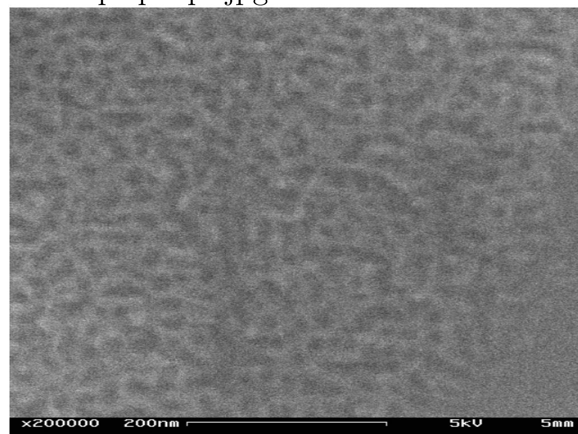

(b) ps-b-pfs-b-ps with inital thickness 26 nm

Figure 2-7: Comparison of PS/PFS diblock and triblock solvent annealed using 10 SCCM toluene or 22 torr toluene.

toluene ps pfs.jpg

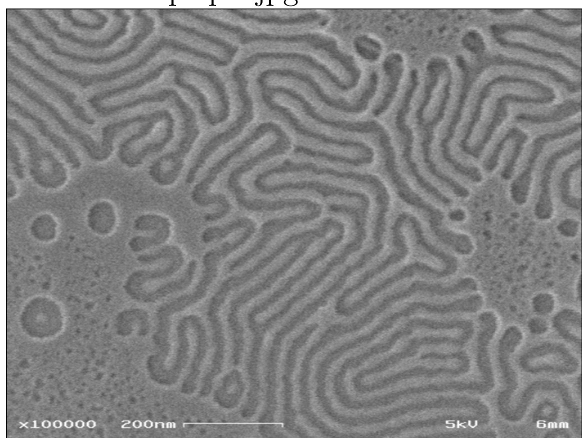

(a) ps-b-pfs inital thickness of 37nm

toluene sfs.jpg

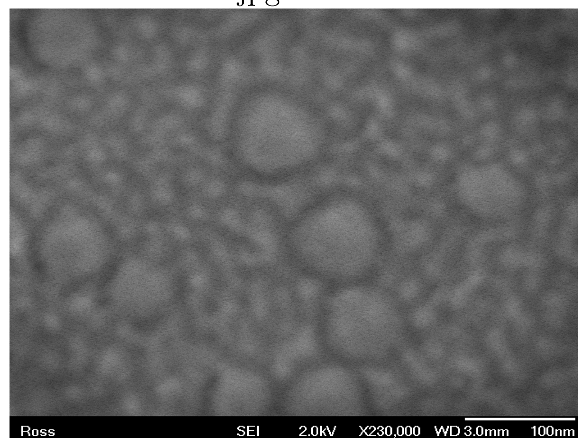

(b) ps-b-pfs-b-ps inital thickness of 26nm

Figure 2-8: Comparison of PS/PFS diblock and triblock solvent annealed using 8 SCCM toluene:1.6 SCCM chloroform:0.4 SCCM nitrogen gas or 17.4 torr toluene:40.9 torr chloroform

toluene ps-pfs.jpg

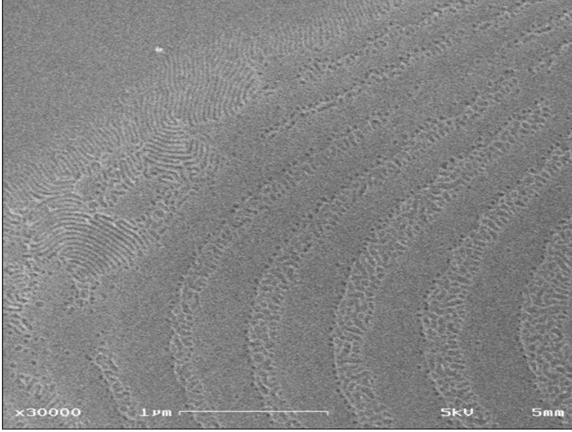

(a) ps-b-pfs inital thickness of 36nm

ps pfs ps.jpg

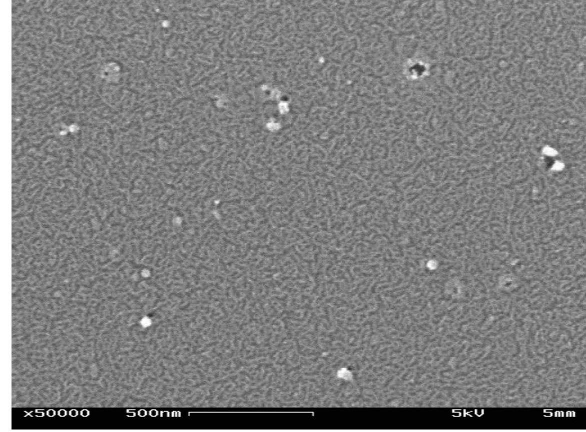

(b) ps-b-pfs-b-ps initial thickness of 26nm

Figure 2-9: Comparison of PS/PFS diblock and triblock solvent annealed using 4 SCCM toluene:4.8 SCCM chloroform: 1.2 SCCM nitrogen gas or 8.5torr toluene:120.4 torr chloroform

chloroform ps pfs.jpg

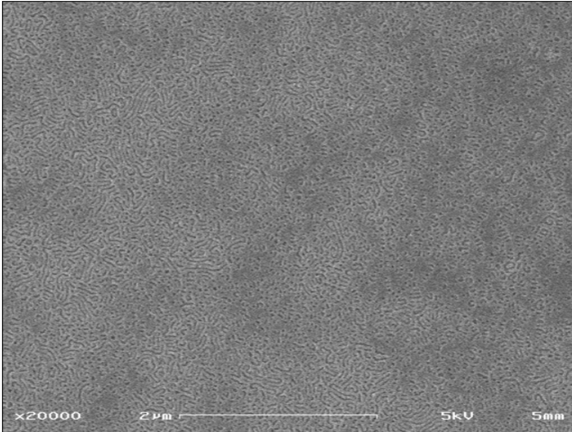

(a) ps-b-pfs inital thickness of 36nm

ps pfs ps.jpg

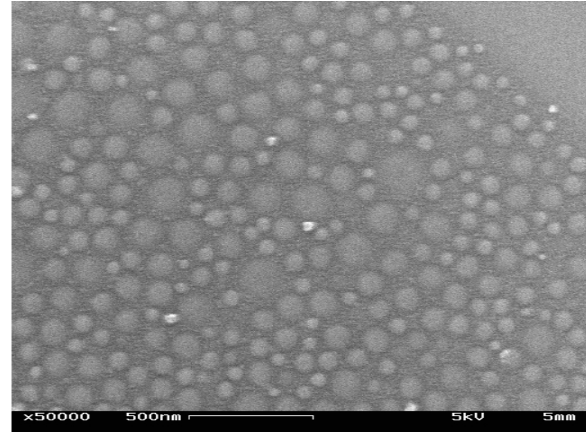

(b) ps-b-pfs-b-ps initial thicnkess of 26nm

Figure 2-10: Comparison of PS/PFS diblock and triblock solvent annealed using 8 SCCM chloroform:2 SCCM nitrogen gas or 196 torr chloroform

greater selectivity for a single block. When comparing our 8 SCCM chloroform to 2 SCCM nitrogen gas solvent annealed diblock sample to a thermally annealed sample, the same morphology is achieved. This tells us that chloroform has low selectivity between PFS and PS. This is consistent with the film thickness measurements from the previous section.

anneal.jpg 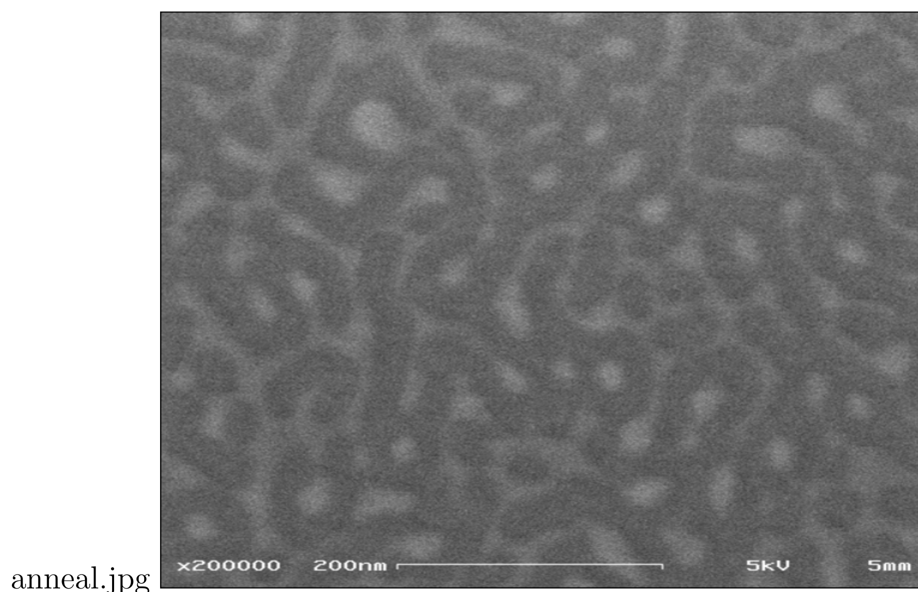

Figure 2-11: 49kg/mol 42% PFS by volume PS-b-PFS sampled thermally annealed.

[1] Ion Bita, Joel K. W. Yang, Yeon Sik Jung, Caroline A. Ross, Edwin L. Thomas, and Karl K. Berggren. Graphoepitaxy of Self-Assembled Block Copolymers on Two-Dimensional Periodic Patterned Templates. Science 15 August 2008: 321 (5891), 939-943

[2] Jin Kon Kim, Seung Yun Yang, Youngmin Lee, Youngsuk Kim. Functional nanomaterials based on block copolymer self-assembly. Progress in Polymer Science 35 (2010) 1325-1349

[3] Rachel A. Segalman. Patterning With Block Copolymer Thin Films. Materials Science and Engineering R 48 (2005) 191-226

[4]Lammertink, R. G. H.; Hempenius, M. A.; van den Enk, J. E.; Chan, V. Z.-H.; Thomas, E. L.; Vancso, G. J. Nanostructured thin films of organic-organometallic block copolymers: One-step lithography with poly(ferrocenylsilanes) by reactive ion etching, Adv. Mater. 2000, 12, 98.

[5] David A. Rider and Ian Manners (2007): Synthesis, SelfAssembly, and Applications of Polyferrocenylsilane Block Copolymers, Polymer Reviews, 47:2, 165-195

[6] Stanley J. Ashcroft, Andrew D. Clayton, and Ronald B. Shearn.Isothermal vapor-liquid equilibriums for the systems toluene-n-heptane, toluene-propan-2-ol, toluene-sulfolane, and propan-2-ol-sulfolane.,Journal of Chemical and Engineering Data 1979 24 (3), 195-199.

[7] Brandrup, J.; Immergut, Edmund H.; Grulke, Eric A.; Abe, Akihiro; Bloch, Daniel R. (1999; 2005). Polymer Handbook (4th Edition).. John Wiley and Sons.

[8] Stimuli-Responsive Gels Based on Ring-Opened Polyferrocenes: Synthesis, Characterization, and Electrochemical Studies of Swellable, Thermally Cross-Linked Polyferrocenylsilanes. Kulbaba, Kevin ; MacLachlan, Mark J. ; Evans, Christopher E. B. ; Manners, Ian Polymer Gels. October 15, 2002, 175-188

Chapter 3

Conclusion

Though we did not achieve the level of long-range ordering that would have been ideal we have shown that future solvent annealing will require solvents with a greater selectivity between the two polymer blocks.Further investigation into alternative brush layers may also be necessary to deter dewetting of our thin films that prevents the use of longer solvent annealing times andfurther ordering. Though the goal of this project was to find a process that would allow us to use PS-b-PFS-b-PS as a precursor for a mask or template material we did find that the triblock produces smaller feature sizes as compared to the diblock.